

Pseudolinear Optical System Reach Enhancement via Runlength-Limited Coding

Vladimir Pechenkin and Frank R. Kschischang, *Fellow, IEEE*

Abstract

This paper demonstrates that the transmission distance of an ON–OFF-keyed high-speed pseudolinear optical communication system can be dramatically improved by means of runlength-limited coding. The key idea is to impose constraints on transmitted sequences such that the minimum interpulse spacing increases, and the average transmission power decreases. Both effects result in considerable suppression of intrachannel four-wave mixing, a major nonlinear penalty in pseudolinear long-haul links. Several coding schemes with different properties are designed for various constraints and compared against a prototypical reference system. Finally, numerical simulations are performed for a benchmark system employing differential phase-shift keying. The results obtained indicate that the runlength-limited coding approach can be considered a legitimate alternative to this more advanced modulation format.

Index Terms

Fiber-optic communications, intrachannel four-wave mixing, runlength-limited coding, differential phase-shift keying.

I. INTRODUCTION

Differential phase-shift keying (DPSK) modulation format is generally believed to be superior to more traditional ON–OFF keying (OOK), both in terms of receiver sensitivity and tolerance to intrachannel nonlinear effects [1]. In this paper, however, we will show that the application of runlength-limited (RLL) coding can significantly extend the reach of ON–OFF-keyed systems and make them competitive with DPSK.

The main idea was already introduced in our earlier work [2]–[5], where a coding scheme for the so-called $(2, \infty)$ constraint was designed and applied to a prototypical fiber-optic link. The transmission distance was kept the same, and the gain from constrained coding was transformed into data rate increases of up to 50%. Here, we look at the same problem from a different and practically more important perspective. In this paper we fix the data rate, and the coding gain is converted into a longer system reach.

The gain itself comes from strong suppression of intrachannel four-wave mixing (IFWM). The latter is a well-known nonlinear effect [6]–[8] that severely limits the reach of long-haul dispersion-managed pseudolinear fiber-optic links operating at channel data rates of 40 Gb/s or higher. IFWM results in complex intersymbol interference and quickly degrades the system performance. From the point of view of IFWM mitigation, shorter optical pulses are known to be preferable, since greater pulse separation weakens the intersymbol interactions [6]. This observation opens the door for a successful application of RLL coding, as will be elaborated on in Section IV. In a few words, imposing RLL constraints on transmitted sequences simultaneously increases the interpulse spacing and decreases the average transmission power, both effects dramatically reducing the intensity of IFWM-induced perturbations. Consequently, optical pulses of higher energy can be used, which improves optical signal-to-noise ratio (OSNR) and ultimately transmutes into a substantial boost in system reach. In our experiments, it was extended by 40–80% depending on the coding scheme applied and the pulse shape utilized.

It should be noted that constrained coding as a method to suppress IFWM has also been proposed in [9]–[12], albeit in a completely different way. The key idea in [9]–[12] is to constrain the transmitted sequences in such a way that certain undesirable

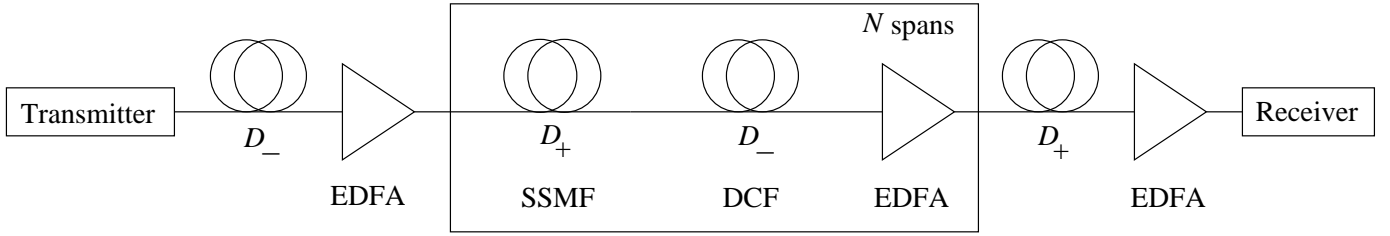


Fig. 1. Dispersion profile of the system. The number of spans is variable.

bit patterns are avoided. However, in order to maintain the data rate required, both the bit slot duration and the interpulse spacing have to be shrunk together. This enhances the intrachannel nonlinear interactions and somewhat diminishes the gain from constrained coding. Despite being very interesting, the approach of [9]–[11] requires further study. Most importantly, [9]–[11] do not provide estimates of the ultimate gain in reach. Also, the potential error propagation effects of practical decoders need to be investigated. In this paper, both issues are addressed.

The remainder of the paper is organized as follows: In Section II, an OOK reference system is set up. In Section III, several RLL codes are constructed, and their properties are discussed. Although the general theory of constrained coding is well developed [13]–[15], we find it useful to emphasize a few important features particularly relevant to our work. The performance of all schemes is analyzed in Section IV, where a significant improvement in system reach is clearly demonstrated. Further comparison against the more advanced DPSK modulation format is the subject of Section V. Section VI summarizes the results and concludes the paper.

II. REFERENCE SYSTEM MODEL

In order to see the benefits of RLL coding, a reasonable “benchmark” or reference system must first be designed. This is the goal of the section. The procedure below is similar to the one followed in [5] although more realistic parameters are used here.

The dispersion map consists of a standard single-mode fiber (SSMF) followed by a dispersion-compensating fiber (DCF). The parameters of both types of fibers are summarized in Table I, the nonlinear Kerr coefficient being $2.6 \times 10^{-20} \text{ m}^2/\text{W}$. Optical amplifiers with noise figure 4.5 dB are inserted every 65 km to fully compensate for fiber loss. The system is thus composed of a series of alternating spans of SSMF and DCF. To reduce the negative impact of both IFWM and IXPM, a segment of DCF of length $L_{\text{pre}} = 2.4 \text{ km}$ was prepended to the link. The length of the postcompensating SSMF was adjusted accordingly to make the average dispersion equal to 0. The entire dispersion profile of the system is schematically depicted in Fig. 1. As in [5], the main design tradeoff is to balance the negative contributions from amplified spontaneous emission (ASE) noise generated by inline optical amplifiers and the intersymbol interference caused by IFWM.

Standard 33% RZ pulses of peak power P_0 are used for the transmission of marks. This is a very popular pulse shape often seen in various studies (e.g., [10]). The corresponding envelope $A_{33}(t)$ may be written as

$$A_{33}(t) = \sqrt{P_0} \cos\left(\frac{\pi}{2} \sin \frac{\pi t}{T_B}\right), \quad (1)$$

and the pulse energy E_0 is computed as $E_0 = P_0 T_B (1 + J_0(\pi))/2$, where $J_0(\pi)$ stands for the Bessel function of the first kind. The bit slot duration is set to $T_B = 24 \text{ ps}$, which corresponds to the symbol rate of about 41.67 GS/s.

The receiver consists of an ideal optical filter with bandwidth $B_o = 4/T_B$, a photodiode with quantum efficiency 0.9, an integrate-and-dump electrical filter and a slicer. In the absence of nonlinear effects, the probability of error p_u can be obtained

	SSMF	DCF
L , km	55.0	10.0
α , dB/km	0.210	0.545
D , ps/(nm·km)	17.0	-93.5
S , ps/(nm ² ·km)	0.058	-0.319
A_{eff} , μm^2	80.0	30.0

TABLE I
DISPERSION MAP PARAMETERS.

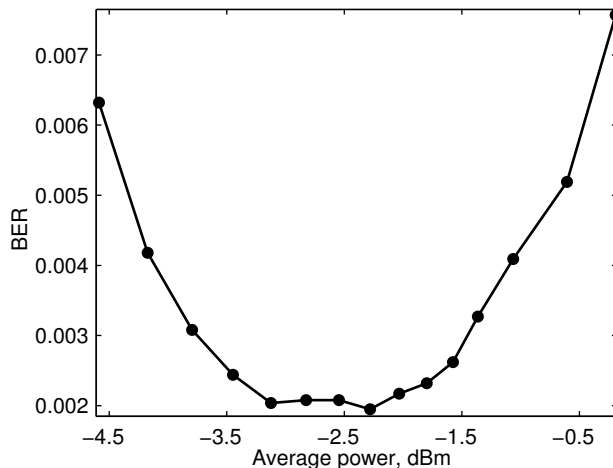


Fig. 2. Probability of error for the OOK reference system as a function of the average transmission power; total transmission distance is 5540.6 km.

analytically [16], [17]. The reference system is required to have $p_u \leq 2 \times 10^{-3}$, and a similar condition is imposed on all the links designed in this paper. Although not necessarily the best operating point from the information theory perspective, this is a popular threshold frequently used in literature to compare lightwave systems employing forward error correction. Our objective is to find the maximum transmission distance L for which the condition $p_u < 0.002$ is satisfied.

Numerical simulations were performed for 2^{15} -bit de Bruijn pseudorandom input sequences with the help of the split-step Fourier method [18]. First, we considered a fully uncoded OOK system. The maximum achievable reach was limited to about 85 amplifier spans (or 5540.6 km). The introduction of alternate mark inversion suppressed the formation of the strongest ghost pulses [19] and allowed the transmission distance to be extended to about 90 amplifier spans (or 5865.6 km). For the sake of illustration, the curves representing the probability of error p_u are plotted for both systems as a function of the average transmission power (Fig. 2 and Fig. 3). Finally, we investigated the application of more advanced phase coding techniques such as the fixed-pattern modulation [20] and $\pi/2$ alternate-phase modulation [21], [22]. The optimization of both the transmission power and the amount of precompensation permitted us to further increase L up to about 6.7 Mm for both approaches.

We now turn our attention to the key contribution of this paper: the application of RLL coding for the sake of extending the system reach. Before that, however, the coding schemes along with their important properties need to be formally introduced.

III. RLL CODE CONSTRUCTION ASPECTS

A binary channel is said to be RLL if transmitted sequences are constrained to have at least d “0”s between any pair of adjacent “1”s. Since the introduction of constraints inevitably decreases the number of possible channel words, the “capacity” C_d of an RLL system with parameter d is always less than 1 bit per channel use. Mathematically, C_d represents the fact that the number of valid constrained sequences of length m grows asymptotically as 2^{mC_d} . The reference system, on the contrary, operates with data streams of equiprobable “0”s and “1”s and, therefore, its capacity is essentially 1.

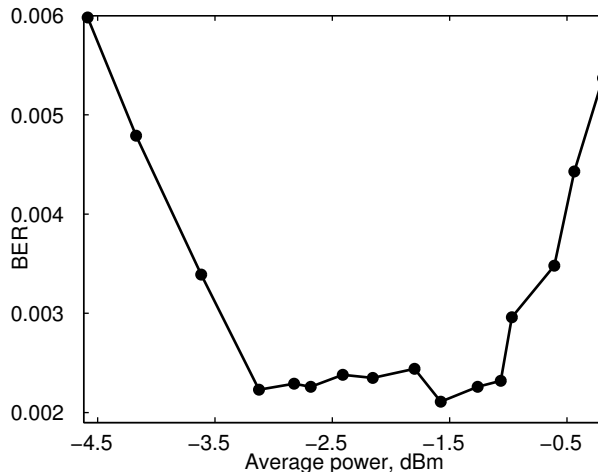


Fig. 3. Probability of error for the OOK-AMI reference system as a function of the average transmission power; total transmission distance is 5865.6 km.

Information transmission through an RLL channel requires a coding scheme that performs two main tasks: it must both unambiguously map arbitrary words into RLL sequences and protect the data from noise. Since the latter problem may be solved by the application of a suitable outer error-correcting code (ECC) available, we consider the former task only.

In this paper, all RLL codes are constructed with the help of the state-splitting algorithm [13]–[15]. Given the d -constraint and a pair of integers k and n satisfying $k/n < C_d$, a finite-state encoding machine with the fixed rate of k/n can be obtained as a result of this well-known procedure. At each time instant, the encoder accepts k input bits and outputs n channel bits, the results also depending on the internal state of the machine governed by the input. Every edge is labelled accordingly.

In the absence of noise, constrained sequences produced by such an encoder may be decoded by a sliding-window demodulator (SWD). Typically, at every clock cycle, the SWD makes a decision about k source bits based on the contents of a decoding window. The size of the window depends on the actual code utilized and usually exceeds n . At the next cycle, the window slides along the received word by n bits, and another decision is made. In general, a few dummy symbols must be appended to each block of data to correctly resolve the uncertainty for the last k bits.

While an SWD is a good practical solution, its implementation is often complicated by the need to design large lookup tables. For example, an SWD for one of the codes considered in this paper requires a window of 16 bits to make a decision about three input bits. In other words, a lookup table with 2^{16} entries must be constructed via some sensible procedure. To avoid such problems, we universally apply the Viterbi decoding algorithm in this paper. Certainly, its application brings up other issues. In particular, the underlying branch metric must be carefully chosen. Ideally, a metric based on the channel statistics is preferable. However, extensive simulations are necessary to obtain such data, and the entire procedure has to be repeated for each dispersion map. For simplicity, Hamming distance is used in this work instead. The performance of such a decoder turns out to be only slightly better than that of the SWD in most cases. Hence, its usage has a negligible impact on our results.

In general, a good RLL code must satisfy several properties. Firstly, its rate $R_d = k/n$ is expected to be a ratio of two small integers. This not only considerably simplifies code construction and reduces the encoding and decoding complexity, but also avoids severe error amplification. Designing constrained codes of high rate, as proposed in [23], may require additional coding layers [24] and quickly become impractical for these very reasons. Secondly, it is desirable that the rate efficiency $\eta_d = R_d/C_d$ be as close to 1 as possible. Unfortunately, if it is the case, it is not always feasible to construct a code with a short decoding window. Consequently, error propagation may not be limited. Hence, a compromise between the two requirements must be

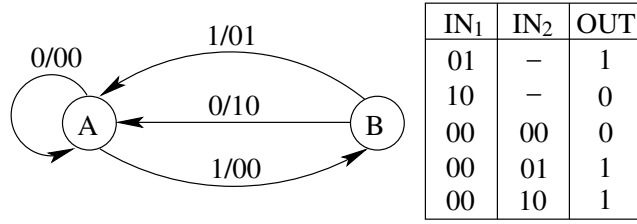


Fig. 4. Encoding machine and decoding table for code C_2 .

d	0	1	2	3	4	4	5
C_d	1.0	0.6942	0.5515	0.4650	0.4057	0.4057	0.3620
code	OOK	C_1	C_2	C_3	C_{41}	C_{42}	C_5
R_d	1.0	2/3	1/2	3/7	3/8	2/5	1/3
$\eta_d, \%$	1.00	96.03	90.67	92.17	92.44	98.60	92.08
q_1	1/2	4/15	1/6	0.1394	0.1123	0.1221	2/21
$2q_1/R_d$	1.0	4/5	2/3	0.6505	0.5989	0.6105	4/7
G_{av}, dB	0.00	0.97	1.76	1.87	2.23	2.14	2.43
T_B, ps	24.0	16.0	12.0	10.28	9.0	9.6	8.0
Δ, ps	24.0	32.0	36.0	41.12	45.0	48.0	48.0
RZ %	33.3	50.0	66.7	77.8	88.9	83.3	100
L, Mm	5.8	8.4	10.3	10.4	10.1	10.1	9.7

d – RLL constraint C_d – RLL capacity R_d – RLL code rate η_d – rate efficiency = R_d/C_d q_1 – probability of a mark	G_{av} – average power savings T_B – bit slot duration Δ – minimum pulse separation RZ% – minimum duty cycle required L – maximum transmission distance
--	--

TABLE II

RLL CODE PARAMETERS AND PROPERTIES.

found.

The code rates R_d used in this work are listed in Table II for different d , along with the corresponding quantities C_d and η_d . (The reader will also find these C_d values in [13, Table 5.4], along with a clear explanation of how these values are derived.) The column with $d = 0$ represents the OOK reference system and is provided to facilitate comparison. Thirdly, the statistical properties of channel sequences must help suppress IFWM. The importance of this factor has been discussed in [3], [5].

In our previous work, we considered $d = 2$ only and compared two coding schemes designed for this particular constraint [5]. The one that was judged to be superior will be used in this paper as well. Its finite-state encoding machine along with the decoding table for the corresponding SWD is presented in Fig. 4.

Here, we will also investigate other RLL constraints in the range from $d = 1$ to $d = 5$. For all constraints except $d = 4$, we design a single scheme that matches the above requirements reasonably well. Each code is assigned a unique label containing a calligraphic C letter and the underlying d -constraint. For $d = 4$, two different high rate schemes are constructed and compared against each other. The most important properties of all the codes are summarized in Table II, while the encoding machines actually used in numerical simulations are presented in the appendix.

IV. RLL CODING FOR OPTICAL CHANNELS

Since any RLL system always transmits less than 1 bit per channel use, this loss in capacity has to be compensated for by speeding the symbol rate up. In other words, the bit slot must be shrunk by a factor of $1/R_d$ to maintain the same data rate. Although this approach appears to be faulty at first glance, it turns out to be superior to the reference system for several reasons.

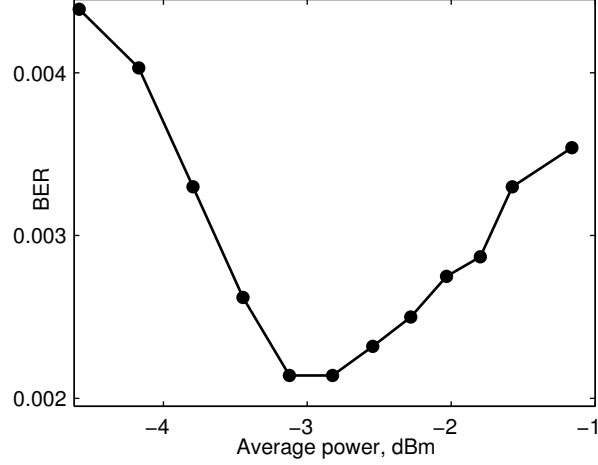


Fig. 5. Probability of error for the DPSK reference system as a function of the average transmission power; total transmission distance is 8335.6 km.

A. The Advantages of Coding

The application of an RLL scheme changes the statistical properties of channel sequences with the following fundamental consequences. First of all, the interpulse spacing Δ for the RLL system becomes $(d + 1)R_dT_B$, which happens to be always greater than T_B , the minimum pulse separation for the underlying reference system (see Table II). This effect alleviates the intersymbol interference caused by IFWM. Moreover, if the pulse energy E_0 is fixed, the RLL system always consumes less average transmission power P_{av} and, therefore, is more tolerant to various nonlinear effects. Indeed, P_{av} can be computed as

$$P_{av} = \frac{q_1 E_0}{R_d T_B}, \quad (2)$$

where q_1 is the probability that a randomly selected channel bit is a “1.” For the reference system ($d = 0$), $R_0 = 1$ and $q_1 = 1/2$ so $P_{av} = E_0/(2T_B)$. For the RLL system, q_1 is an important quantity related to the distribution of constrained sequences. It can be calculated directly from the encoder graph via treating it as a Markov chain. The procedure is straightforward but somewhat lengthy so only the results are summarized in Table II. In all cases, q_1 is a rational number, but an approximation is given where the exact fraction is too cumbersome. Clearly, the quantity $2q_1/R_d < 1$ for all schemes considered here and, therefore, all RLL systems operate at lower P_{av} for the same E_0 . For the sake of completeness, power savings in dB with respect to the reference system, G_{av} , is also shown.

The increase of Δ and the simultaneous decrease of P_{av} represent two crucial advantages of the RLL system, since both effects greatly reduce the intensity of IFWM-induced perturbations, with little or no penalty in OSNR. An additional benefit may also be provided by an accurate design of the coding scheme. As was pointed out in [5], the most troublesome sequences leading to the formation of the strongest ghost pulses may sometimes be eliminated in the code construction process.

B. Simulation Results

We simulate RLL links in a straightforward manner. All major parameters specified in Section II remain unchanged with the only exception. Unlike our previous work [5] where exactly the same pulse shape was utilized for both the reference and the constrained system, here we employ optical pulses of different shapes. Intuitively, it makes sense to cut off the tails that extend far into the neighboring “0” bit slots and transmit more “compact” signals. The only restriction imposed is that the FWHM must be no less than 8 ps to approximately preserve the spectral efficiency. For example, standard 50% RZ may be

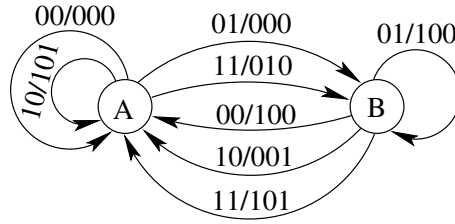


Fig. 6. Encoding machine for code C_1 .

used for C_1 and 67% CSRZ – for C_2 . For C_3 , the minimum duty cycle is 78%, although any fraction between 78% and 100% is possible, in principle. Similarly, code C_{41} requires at least 89% duty cycle, while the modulation format has to become NRZ for C_5 . Explicit expressions for all pulse shapes used in simulations are presented in the appendix. It should be noted that since $C_6 \approx 0.3282 < 1/3$, no coding scheme is capable of providing $\text{FWHM} \geq 8$ ps, while still maintaining the data rate. Hence, $d \geq 6$ is not considered in this paper.

No phase coding is applied except for C_1 . As observed in [5], AMI is not helpful for C_2 , since the worst bit patterns have already been eliminated by the code construction. On the contrary, such sequences occur relatively frequently in C_1 , and, therefore, AMI is expected to be beneficial in this case. In our simulations, it did extend the system reach by 5–6 amplifier spans.

The probability of error p_c is estimated by counting the number of errors detected at the output of the RLL decoder. To establish a fair comparison against the reference system, the condition $p_c \leq 0.002$ is imposed. For all schemes, the maximum transmission distance L we were able to attain is recorded in Table II. A quick glance at the results is enough to see that all RLL codes dramatically improve the reach of the reference system. Code C_1 is the least powerful, while all the other schemes are capable of approaching or breaking the 10 Mm barrier. Somewhat surprisingly, for $d \geq 2$, the performance of all codes is quite comparable. Even the schemes with the most complex encoders and the longest decoding windows appear to be quite resilient to channel perturbations.

V. COMPARISON WITH DPSK

An intriguing question remaining is whether RLL coding can compete with the powerful DPSK modulation format, which has been demonstrated to be superior to OOK at 40 Gb/s. Certainly, extensive testing for a variety of setups and parameters is required before a reasonable conclusion can be drawn. Here, we will only scratch the surface of this problem. In particular, the transmitted pulse shape remains the same as for the OOK reference system, i.e, standard 33% RZ. For simplicity, both the receiver filters and the dispersion map are also preserved. Only the balanced receiver structure [1] is considered, since it is an integral part of the DPSK success.

Numerical simulations confirm that the system reach up to 128 amplifier spans (or 8435.6 km) is achievable, a dramatic improvement with respect to the OOK reference system. Despite a longer transmission distance, the optimum P_{av} is around -3 dBm (Fig. 5), which is close to the best operating point for the OOK system. Nevertheless, the results in Table II indicate that this is only comparable to C_1 , the least powerful coding scheme considered in this paper.

In principle, the DPSK system reach can be improved by adjusting the amount of precompensation. For example, if $L_{\text{pre}} = 2.0$ km or $L_{\text{pre}} = 1.8$ km, the transmission distance of 139 amplifier spans (9048 km) is attainable. Somewhat surprisingly, this is still insufficient to surpass the performance of the RLL-coded systems. Further modifications of the dispersion map would require a considerable amount of simulation time but definitely represents an important research problem to investigate.

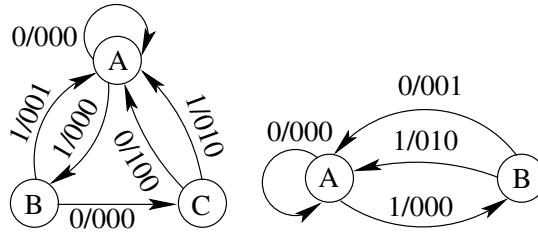


Fig. 7. Encoding machines for C_5 . An encoder of rate $1/3$ code for $d = 4$ (with two states) is also shown for comparison.

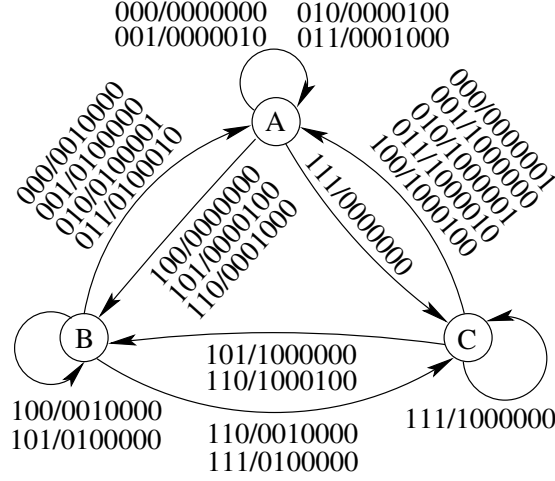


Fig. 8. Encoding machine for code C_3 . Multiple transition between states are represented by a single edge for clarity.

VI. DISCUSSION AND CONCLUSION

In this paper, we applied runlength-limited coding to high-speed long-haul pseudolinear optical data transmission systems limited by IFWM. A number of schemes were designed and their performance was investigated in the context of a realistic fiber-optic system. We showed that the RLL method efficiently suppresses the ghost pulse formation and is capable of extending the OOK system reach by as much as 40–80%. Moreover, our simulation results indicate that even a more sophisticated DPSK modulation format may not be able to measure up to the coded system performance.

It should be stressed that our approach is fundamentally different from the original idea behind RLL coding. In recording systems, the “transmission distance” simply does not exist, and the d -constraint is introduced solely for the purpose of increasing the data storage density. In our work, the data rate is preserved, which dramatically improves the underlying physical channel and allows the system reach to be significantly extended.

Several issues deserve further comments.

We found it essential that an RLL system be judged by the probability error estimated at the output of the RLL decoder and not by means of standard but “indirect” quantities. For example, the Q -factor estimated from the eye diagram at the output of the optical filter was very poorly correlated with the probability of error actually observed. This may be explained by the fact that every RLL decoder has a particular “behavior” and affects the statistics of the physical channel differently. In other words, resilience to channel errors and the error amplification factor are individual characteristics of the decoder.

Hardware implementation of the proposed systems does not seem to be prohibitively complex. The major cost involves a speedup of the electronics by a factor of $1/R_d$, while the actual realization of the RLL encoders and decoders appears to be straightforward. The choice of the code will definitely depend on a number of factors and is a separate research problem. Our intuition suggests that C_2 is probably the optimum scheme to utilize in practice, when all the requirements are considered

together.

In principle, the transmission distance can be further extended by optimizing the FEC threshold p_u . The value of 0.002 used in this paper is not necessarily the optimum one, and better results might be possible if $p_u > 0.002$ is allowed. Such an approach makes perfect sense from the information theory point view but definitely requires more powerful and more complex error-correcting codes.

It is important to note that the ultimate test of the RLL coding approach is its application to wavelength-division-multiplexed (WDM) systems. It is conceivable that the gain obtained from the suppression of the intrachannel impairments can potentially be traded off to relieve the impact of the intrachannel crosstalk. For example, wider optical pulses may reduce the crosstalk but enhance IFWM at the same time. Designing such a WDM system is a challenging but at the same time exciting research topic.

APPENDIX

Here, we will provide the details of all RLL systems implemented in this work. Since Viterbi decoding algorithm is utilized at the receiver, each coding scheme may be fully described by its finite-state encoding machine.

The encoder for \mathcal{C}_1 (Fig. 6) is already well known in the literature (see, e.g., [25]). Its decoding table is straightforward to construct but it is somewhat long and thus omitted here. The encoding machine for \mathcal{C}_5 is presented in Fig. 7. The graphs for \mathcal{C}_3 (Fig. 8) and \mathcal{C}_{41} (Fig. 9) are more complex but it is only due to a greater number of edges. All the encoders are still very simple, none of them having more than three states. Not surprisingly, the scheme having the highest rate efficiency (\mathcal{C}_{42}) also possesses the most complicated encoding machine with 7 states (Fig. 10), but it is still a reasonable number.

In each case, the pulse shape used for transmission of “1”s is selected based on the minimum duty cycle required, which is specified in Table II. In particular, the system based on \mathcal{C}_1 utilized standard 50% RZ:

$$A_{50}(t) = \sqrt{P_0} \cos \left(\frac{\pi}{4} \cos \frac{2\pi t}{T_B} - \frac{\pi}{4} \right). \quad (3)$$

Similarly, standard 67% CSRZ was chosen for \mathcal{C}_2 :

$$A_{67}(t) = \sqrt{P_0} \sin \left(\frac{\pi}{2} \cos \frac{\pi t}{T_B} \right), \quad (4)$$

although the carrier was actually not suppressed in this case. For longer pulse durations, we adopted a model from [26]. An optical pulse having peak power P_0 and duty cycle a , $0.5 < a < 1$, is represented as

$$A(t) = \begin{cases} \sqrt{P_0} \sin \left(\frac{\pi t}{2(1-a)T_B} \right), & t \in [0, (1-a)T_B] \\ \sqrt{P_0}, & t \in [(1-a)T_B, aT_B] \\ \sqrt{P_0} \cos \left(\frac{\pi(t-aT_B)}{2(1-a)T_B} \right), & t \in [aT_B, T_B]. \end{cases} \quad (5)$$

The NRZ modulation format necessary for \mathcal{C}_5 utilizes a similar waveform:

$$A(t) = \begin{cases} \sqrt{P_0} \sin \left(\frac{\pi a t}{2(1-a)T_B} \right), & t \in [0, (1-a)T_B/a] \\ \sqrt{P_0}, & t \in [(1-a)T_B/a, T_B] \\ \sqrt{P_0} \cos \left(\frac{\pi a(t-T_B)}{2(1-a)T_B} \right), & t \in [T_B, T_B/a]. \end{cases} \quad (6)$$

Here, $0.5 < a < 1$ may be selected arbitrarily. In our experiments, we set $a = 0.8$.

ACKNOWLEDGEMENT

The authors would like to thank Alan Pak Tao Lau for valuable discussions.

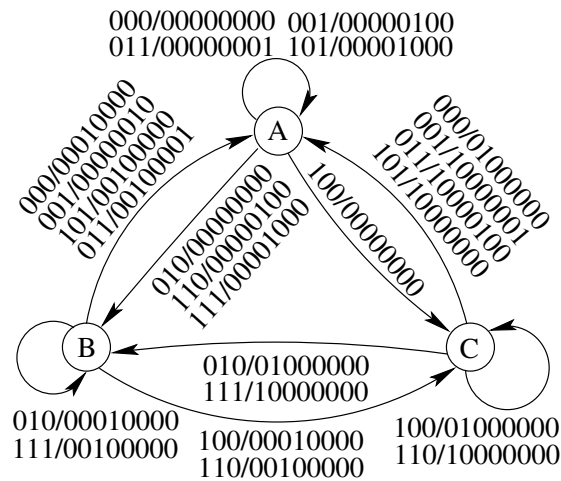


Fig. 9. Encoding machine for code C_{41} . Multiple transition between states are represented by a single edge.

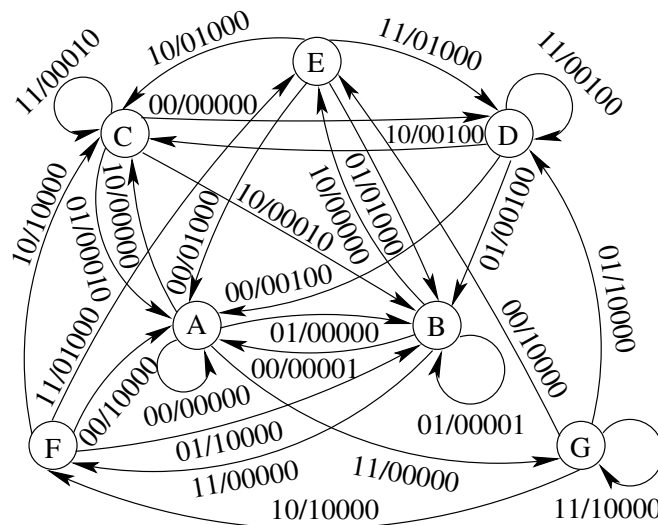


Fig. 10. Encoding machine for code C_{42} .

REFERENCES

- [1] A. H. Gnauck and P. J. Winzer, "Optical phase-shift-keyed transmission," *J. of Lightwave Tech.*, vol. 23, no. 1, pp. 115–130, Jan. 2005.
- [2] V. Pechenkin and F. R. Kschischang, "Higher bit rates for quasi-linear optical data transmission systems via constrained coding," in *Proc. OFC*, Anaheim, CA, USA, Mar. 2006, paper JThB7.
- [3] —, "Ghost pulse suppression in quasi-linear optical data transmission systems via constrained coding," in *Proc. of 23rd Biennial Symp. Commun.*, Kingston, Ontario, Canada, Jun. 2006, pp. 88–91.
- [4] —, "Constrained coding for WDM systems," in *Proc. of European Conf. Optical Communication*, Cannes, France, Sep. 2006, paper Th2.6.4.
- [5] —, "Constrained coding for quasi-linear optical data transmission systems," *J. of Lightwave Tech.*, vol. 24, no. 12, pp. 4895–4902, Dec. 2006.
- [6] A. Mecozzi, C. B. Clausen, and M. Shtaif, "Analysis of intrachannel nonlinear effects in highly dispersed optical pulse transmission," *IEEE Photonics Tech. Letters*, vol. 12, no. 4, pp. 392–394, Apr. 2000.
- [7] P. Johannisson, D. Anderson, A. Berntson, and J. Mårtensson, "Generation and dynamics of ghost pulses in strongly dispersion-managed fiber-optic communication systems," *Optics Letters*, vol. 26, no. 16, pp. 1227–1229, Aug. 2001.
- [8] M. J. Ablowitz and T. Hirooka, "Resonant intrachannel pulse interactions in dispersion-managed transmission systems," *IEEE J. of Select. Topics in Quantum Electronics*, vol. 8, no. 3, pp. 603–615, May/June 2002.
- [9] I. B. Djordjevic and B. Vasic, "Constrained coding techniques for the suppression of intrachannel nonlinear effects in high-speed optical transmission," *J. of Lightwave Tech.*, vol. 24, no. 1, pp. 411–419, Jan. 2006.
- [10] I. B. Djordjevic, S. K. Chilappagari, and B. Vasic, "Suppression of intrachannel nonlinear effects using pseudoternary constrained codes," *J. of Lightwave Tech.*, vol. 24, no. 2, pp. 769–774, Feb. 2006.
- [11] I. B. Djordjevic, B. Vasic, and V. S. Rao, "Rate 2/3 modulation code for suppression of intrachannel nonlinear effects in high-speed optical transmission," *Proc. IEE-Optoelectronics*, vol. 153, no. 2, pp. 87–92, Apr. 2006.
- [12] N. Kashyap, P. H. Siegel, and A. Vardy, "Coding for the optical channel: the ghost-pulse constraint," *IEEE Trans. Information Theory*, vol. 52, no. 1, pp. 64–77, Jan. 2006.
- [13] K. A. S. Immink, *Coding Techniques for Digital Recorders*. Prentice Hall International (UK) Ltd., 1991.
- [14] B. H. Marcus, P. H. Siegel, and J. K. Wolf, "Finite-state modulation codes for data storage," *IEEE J. Select. Areas Commun.*, vol. 10, no. 1, pp. 5–37, Jan. 1992.
- [15] D. Lind and B. Marcus, *An Introduction to Symbolic Dynamics and Coding*. Cambridge: Cambridge University Press, 1995.

- [16] D. Marcuse, "Derivation of analytical expressions for the bit-error probability in lightwave systems with optical amplifiers," *J. of Lightwave Tech.*, vol. 8, no. 12, pp. 1816–1823, Dec. 1990.
- [17] P. A. Humblet and M. Azizoglu, "On the bit error rate of lightwave systems with optical amplifiers," *J. of Lightwave Tech.*, vol. 9, no. 11, pp. 1576–1582, Nov. 1991.
- [18] O. V. Sinkin, R. Holzlöhner, J. Zweck, and C. R. Menyuk, "Optimization of the split-step Fourier method in modeling optical-fiber communication systems," *J. of Lightwave Tech.*, vol. 21, no. 1, pp. 61–68, Jan. 2003.
- [19] X. Liu, X. Wei, A. H. Gnauck, C. Xu, and L. K. Wickham, "Suppression of intrachannel four-wave-mixing-induced ghost pulses in high-speed transmission by phase inversion between adjacent marker blocks," *Optics Letters*, vol. 27, no. 13, pp. 1177–1179, Jul. 2002.
- [20] M. Zou, M. Chen, and S. Xie, "Suppression of ghost pulses in 40Gbps optical transmission systems with fixed-pattern phase modulation," *Optics Express*, vol. 13, no. 7, pp. 2251–2255, Apr. 2005.
- [21] M. Forzati, J. Mårtensson, A. Berntson, A. Djupsjöbacka, and P. Johannisson, "Reduction of intrachannel four-wave mixing using the alternate-phase RZ modulation format," *IEEE Photonics Tech. Letters*, vol. 14, no. 9, pp. 1285–1287, Sep. 2002.
- [22] D. M. Gill, X. Liu, X. Wei, S. Banerjee, and Y. Su, " $\pi/2$ alternate-phase ON-OFF keyed 40-Gb/s transmission on standard single-mode fiber," *IEEE Photonics Tech. Letters*, vol. 15, no. 12, pp. 1776–1778, Dec. 2003.
- [23] M. Lefrançois, G. Charlet, P. Tran, H. Mardoyan, and S. Bigo, "Improvement of tolerance to nonlinearities resulting from small sequence modifications in 40-Gb/s optical transmission," in *Proc. of European Conf. Optical Communication*, Cannes, France, Sep. 2006, paper Th3.2.4.
- [24] K. A. S. Immink, "A practical method for approaching the channel capacity of constrained channels," *IEEE Trans. Information Theory*, vol. 43, no. 5, pp. 1389–1399, Sep. 1997.
- [25] P. H. Siegel, "Recording codes for digital magnetic storage," *IEEE Trans. Magnetics*, vol. MAG-21, no. 5, pp. 1344–1349, Sep. 1985.
- [26] P. J. Winzer, M. Pfennigbauer, M. M. Strasser, and W. R. Leeb, "Optimum filter bandwidths for optically preamplified NRZ receivers," *J. of Lightwave Tech.*, vol. 19, no. 9, pp. 1263–1273, Sep. 2001.